Published OnlineFirst November 12, 2013; DOI: 10.1158/0008-5472.CAN-13-1196

Priority Report

Cancer Research

Tumor Hypoxia Does Not Drive Differentiation of Tumor-Associated Macrophages but Rather Fine-Tunes the M2-like Macrophage Population

Damya Laoui[1,2], Eva Van Overmeire[1,2], Giusy Di Conza[5], Chiara Aldeni[5], Jiri Keirsse[1,2], Yannick Morias[1,2], Kiavash Movahedi[1,2], Isabelle Houbracken[3], Elio Schouppe[1,2], Yvon Elkrim[1,2], Oussama Karroum[4], Bénédicte Jordan[4], Peter Carmeliet[6], Conny Gysemans[7], Patrick De Baetselier[1,2], Massimiliano Mazzone[5], and Jo A. Van Ginderachter[1,2]

Abstract

Tumor-associated macrophages (TAM) are exposed to multiple microenvironmental cues in tumors, which collaborate to endow these cells with protumoral activities. Hypoxia, caused by an imbalance in oxygen supply and demand because of a poorly organized vasculature, is often a prominent feature in solid tumors. However, to what extent tumor hypoxia regulates the TAM phenotype *in vivo* is unknown. Here, we show that the myeloid infiltrate in mouse lung carcinoma tumors encompasses two morphologically distinct CD11b^{hi}F4/80^{hi}Ly6C^{lo} TAM subsets, designated as MHC-II^{lo} and MHC-II^{hi} TAM, both of which were derived from tumor-infiltrating Ly6C^{hi} monocytes. MHC-II^{lo} TAM express higher levels of prototypical M2 markers and reside in more hypoxic regions. Consequently, MHC-II^{lo} TAM contain higher mRNA levels for hypoxia-regulated genes than their MHC-II^{hi} counterparts. To assess the *in vivo* role of hypoxia on these TAM features, cancer cells were inoculated in prolyl hydroxylase domain 2 (*PHD2*)-haplodeficient mice, resulting in better-oxygenated tumors. Interestingly, reduced tumor hypoxia did not alter the relative abundance of TAM subsets nor their M2 marker expression, but specifically lowered hypoxia-sensitive gene expression and angiogenic activity in the MHC-II^{lo} TAM subset. The same observation in PHD2$^{+/+}$ → PHD2$^{+/-}$ bone marrow chimeras also suggests organization of a better-oxygenized microenvironment. Together, our results show that hypoxia is not a major driver of TAM subset differentiation, but rather specifically fine-tunes the phenotype of M2-like MHC-II^{lo} TAM. *Cancer Res; 74(1); 24–30. ©2013 AACR.*

Introduction

Tumors are often highly infiltrated with inflammatory cells, such as tumor-associated macrophages (TAM). TAM are characterized by plasticity and versatility and may contribute to tumor progression via several mechanisms, including induction of angiogenesis, remodeling of the extracellular matrix, stimulation of cancer cell proliferation and metastasis, and the inhibition of adaptive immunity (1, 2).

Authors' Affiliations: [1]Laboratory of Myeloid Cell Immunology, VIB; [2]Laboratory of Cellular and Molecular Immunology; [3]Cell Differentiation Unit, Diabetes Research Centre, Vrije Universiteit Brussel; [4]Biomedical Magnetic Resonance Unit, U.C. Louvain, Brussels; [5]Laboratory of Molecular Oncology and Angiogenesis; [6]Laboratory of Angiogenesis and Neurovascular Link, Vesalius Research Center, VIB; and [7]Experimental Medicine and Endocrinology, Department of Experimental Medicine, K.U. Leuven, Leuven, Belgium

Note: Supplementary data for this article are available at Cancer Research Online (http://cancerres.aacrjournals.org/).

Corresponding Author: Jo A. Van Ginderachter, Laboratory of Cellular and Molecular Immunology, VIB-Vrije Universiteit Brussel, Building E8, Pleinlaan 2, B-1050 Brussels, Belgium. Phone: 32-2-6291978; Fax: 32-2-6291981; E-mail: jvangind@vub.ac.be

doi: 10.1158/0008-5472.CAN-13-1196

These different functions are exhibited by distinct TAM subpopulations, residing in distinct tumor microenvironments (3, 4). In this context, it has been observed in several tumor models that macrophages can infiltrate both oxygenized perivascular regions as well as hypoxic tumor areas (4–7). Importantly, strong tumor hypoxia and a high density of hypoxic TAM have been shown to correlate with a decreased survival rate (8). Although hypoxia can influence monocyte migration and macrophage proliferation and polarization (9–12), the precise role of tumor hypoxia in intratumoral monocyte differentiation and in shaping the molecular and functional TAM phenotype remains largely unexplored.

In this study, we used prolyl hydroxylase domain 2 (*PHD2*)-haplodeficient mice to evaluate the impact of tumor hypoxia on M2-like MHC-II^{lo} and M1-like MHC-II^{hi} TAM subpopulations, which both differentiate from Ly6C^{hi} monocytes but reside in strongly hypoxic and less hypoxic regions, respectively. The oxygen-sensing PHD2 protein targets hypoxia-inducible transcription factors (HIF) for degradation. Hence, its haplodeficiency creates a "genetic" type of hypoxia, resulting in tumor vessel normalization and tumor oxygenation (13). Using *PHD2*$^{+/-}$ tumors, we demonstrated that hypoxia does not govern TAM subset differentiation and polarization, but regulates hypoxia-sensitive genes and angiogenic activity

Published OnlineFirst November 12, 2013; DOI: 10.1158/0008-5472.CAN-13-1196

specifically in MHC-II^{lo} TAM. Moreover, the diminished hypoxic signature of MHC-II^{lo} TAM is recapitulated in *PHD2*$^{+/+}$ → *PHD2*$^{+/-}$ bone marrow chimeras, illustrating that a better-oxygenized microenvironment drives this phenomenon.

Materials and Methods

More detailed materials and methods can be found in the supplementary material.

Mice, cell line, and tumor models

Female C57BL/6 mice were from Janvier. *PHD2*$^{+/-}$ and *Cx3cr1*$^{gfp/+}$ mice were provided by Peter Carmeliet (VIB-KULeuven) and Frank Tacke (Aachen University), respectively. Procedures followed the guidelines of the Belgian Council for Laboratory Animal Science.

Mice were injected subcutaneously with 3×10^6, or orthotopically with 5×10^5, 3LL-R Lewis lung carcinoma cells.

Tumor preparation, flow cytometry, and cell sorting

Tumor single-cell suspensions from subcutaneous and orthotopic 3LL-R tumors and sorted TAM were prepared as described (4). Commercial antibodies for cell surface stainings are listed in Supplementary Table S1. To prevent aspecific binding, TAMs were preincubated with rat anti-mouse CD16/CD32 (clone 2.4G2; BD Biosciences).

To purify TAM or tumor-associated dendritic cells (TADC), cells were sorted using a BD FACSAria II (BD Biosciences) from 6 to 8 pooled tumors. To purify splenic conventional dendritic cells (DC), spleens were flushed with 200 U/mL collagenase III (Worthington) and squashed. Subsequently, CD11c$^+$ cells were enriched via MACS, using anti-CD11c microbeads (Miltenyi Biotec), after which CD11c$^+$MHC-II^{hi}B220$^-$Ly6C$^-$ DCs were sorted using a BD FACSAria II. Normalized delta-median fluorescence intensity (ΔMFI) was calculated as: [(MFI iNOS staining) − (MFI isotype staining)]/(MFI iNOS staining). FACS data were acquired using a BD FACSCanto II (BD Biosciences).

RNA extraction, cDNA preparation, and quantitative real-time PCR

These experiments were performed as described (4). RNA was extracted using TRIzol (Invitrogen) and was reverse-transcribed with oligo(dT) and SuperScript II RT (Invitrogen). Quantitative real-time PCR (qRT-PCR) was performed in an iCycler, with iQ SYBR Green Supermix (Bio-Rad). Primer sequences are listed in Supplementary Table S2. PCR cycles consisted of 1′ 94°C, 45″ 55°C, 1′ 72°C. Gene expression was normalized using ribosomal protein S12 (*Mrps12*) as a housekeeping gene.

Measurement of arginase activity, NO, and interleukin-10 production

The arginase activity in the lysate of 5×10^5 sorted TAM or TADC was measured as described (4) and NO_2^- was quantified by a Griess reaction (4). Interleukin (IL)-10 concentrations were measured by Bio-Plex (Bio-Rad), according to the supplier's protocols.

Statistics

Significance was determined by the Student *t* test, using GraphPad Prism 4.0 software.

Results

Lung carcinomas are highly infiltrated with a heterogeneous myeloid cell compartment

To study the impact of hypoxia on tumor-associated macrophages, we investigated established subcutaneous 3LL-R tumors with an average tumor volume of 869 ± 75 mm^3. These tumors possessed hypoxic areas, as demonstrated by pimonidazole staining (Fig. 1A), and are highly infiltrated by CD11b^{hi} myeloid cells (51.7 ± 10.8% of the tumor single-cell suspension; Fig. 1B). The myeloid infiltrate encompassed Ly6G^{hi} neutrophils (12.0 ± 3.5% within CD11b^{hi} cells) and different mononuclear phagocyte subsets in various stages of differentiation: Ly6C^{hi}CCR2^{hi}CX$_3$CR1^{int}MHC-II^{neg} monocytes (gate 1; Fig. 1B), Ly6C^{int}CCR2^{lo}CX$_3$CR1^{int}MHC-II^{lo} immature macrophages (gate 2), Ly6C$^{hi/int}$CCR2^{lo}CX$_3$CR1^{int}MHC-II^{hi} immature macrophages (gate 3), Ly6C^{lo}CCR2^{neg}CX$_3$CR1^{lo}MHC-II^{lo} tumor-associated macrophages (MHC-II^{lo} TAM, gate 4), Ly6C^{lo}CCR2^{lo}CX$_3$CR1^{hi}MHC-II^{hi} tumor-associated macrophages (MHC-II^{hi} TAM, gate 5), and Ly6C^{lo}CCR2^{neg}CX$_3$CR1^{hi}MHC-II^{hi} tumor-associated DC (TADC, gate 6). All macrophage subsets showed a high expression of F4/80 and a typical macrophage scatter profile, whereas the TADC expressed higher levels of MHC-II, CD11c, costimulatory, and antigen-presenting molecules, but lower F4/80, CD64, and MerTK (Fig. 1C and Supplementary Fig. S1A), in combination with a characteristic DC morphology (Fig. 1B). In a mixed leukocyte reaction, both TAM subsets were poor stimulators of naive CD4$^+$ and CD8$^+$ T cells compared with TADC, which are equally potent antigen-presenting cells as splenic conventional DC (Fig. Supplementary S1B and S1C). Moreover, at higher cell densities both TAM subsets suppress T-cell proliferation (Supplementary Fig. S1B and S1C).

MHC-II^{lo} and MHC-II^{hi} TAM were morphologically distinct (Fig. 1B), suggestive of a different activation state. In agreement with this notion, enhanced protein expression of prototypic M2-associated markers such as MMR, IL-4Rα, SR-A, stabilin-1, arginase-1, and IL-10 and reduced iNOS activity illustrate the more M2-like nature of MHC-II^{lo} TAM as compared with MHC-II^{hi} TAM (Fig. 1C and D).

To extrapolate these findings to orthotopically grown tumors, 3LL-R was injected intrathoracically. Orthotopic lung tumors contained similar myeloid cell subsets, except for TADC (Supplementary Fig. S2A), with similar M1-like versus M2-like profiles for the MHC-II^{hi} and MHC-II^{lo} TAM, respectively (Supplementary Fig. S2B). Notably, the proportion of distinct lung monocyte and macrophage populations was largely comparable between peritumoral normal lung tissue and naive lungs (Supplementary Fig. S2C).

MHC-II^{lo} and MHC-II^{hi} TAM are derived from the same monocyte precursor but reside in differentially oxygenized tumor regions

TAM subsets could be different because they are derived from distinct monocyte precursors or because they are subject

Published OnlineFirst November 12, 2013; DOI: 10.1158/0008-5472.CAN-13-1196

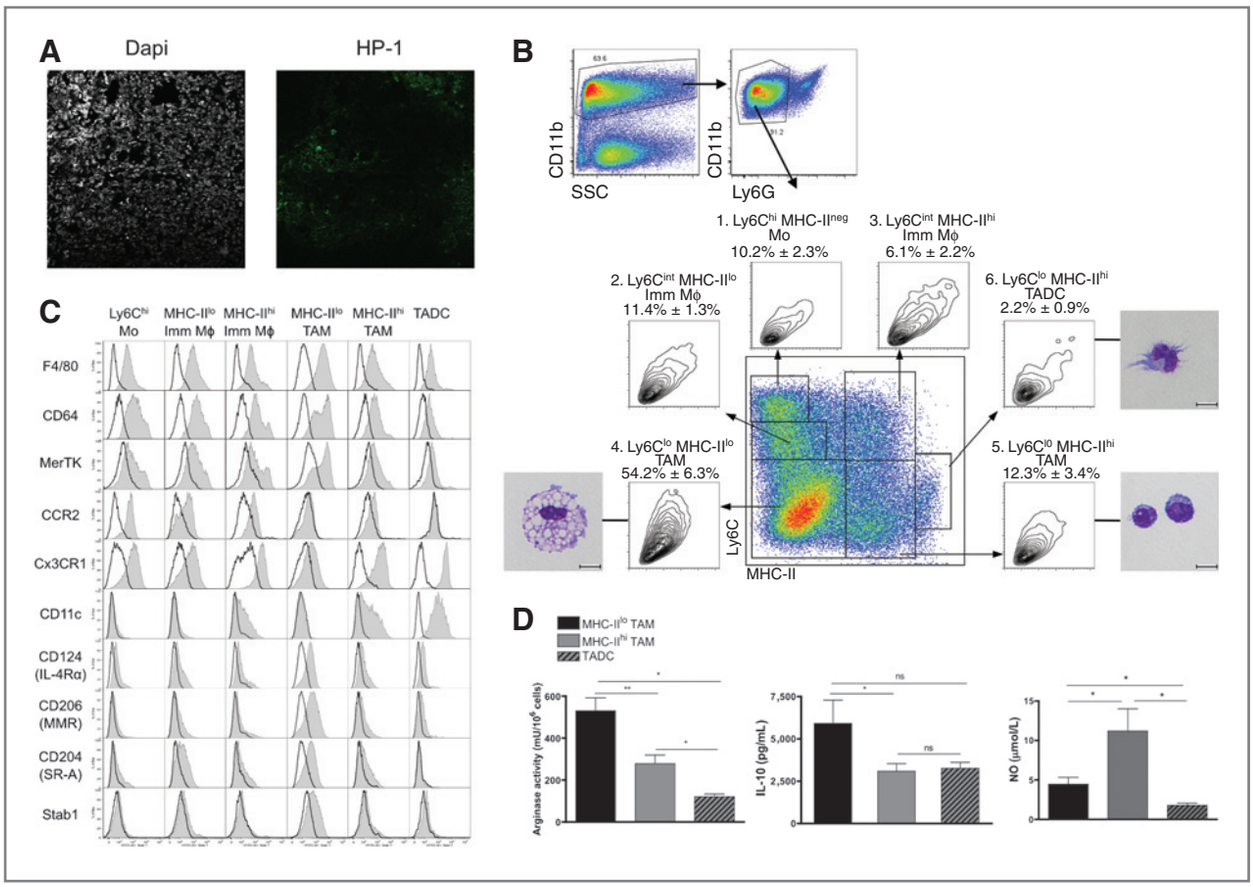

Figure 1. 3LL-R tumors are hypoxic and infiltrated by distinct mononuclear phagocyte subsets. A, frozen tumor sections from HP-1–injected mice were stained for HP-1 adducts and DAPI. B, single-cell suspensions of 13-day-old 3LL-R tumors were stained for the indicated markers. Percentages represent the mean ± SD within the $CD11b^+Ly6G^-$ population. Forward scatter versus side scatter plots and cytospins (scale bar, 10 μm) or histogram overlays (C) are shown. Shaded histogram, expression of the indicated marker; black line, isotype control. D, arginase enzymatic activity was measured in lysates of 5×10^5 sorted TAM or TADC. Spontaneous IL-10 and NO production was measured upon 48 hours *in vitro* culture (3×10^5 TAM or TADC per 200 μL medium). Graphs show mean ± SEM. *, $P < 0.05$; **, $P < 0.01$. All experiments, $n \geq 6$.

to distinct microenvironments. $Ly6C^{lo}CX_3CR1^{hi}$ monocytes are nearly undetectable at the tumor site (data not shown). Moreover, selective labeling of $Ly6C^{hi}$ or $Ly6C^{lo}$ monocytes in the circulation and subsequent tracing of labeled monocyte progeny in the tumor illustrated that exclusively $Ly6C^{hi}$ monocytes give rise to both TAM populations (Fig. 2A). Furthermore, continuous administration of BrdU to the drinking water demonstrated that tumor-infiltrating $Ly6C^{hi}$ monocytes and both immature macrophage populations, all of which do not proliferate as illustrated by cell-cycle analysis (data not shown), rapidly become >90% $BrdU^+$, suggesting these cells are differentiation intermediates with a fast turnover rate (Fig. 2B). Notably, immature macrophages show a lag phase of BrdU incorporation relative to the $Ly6C^{hi}$ monocytes (at 24 hours: 72,5% $BrdU^+Ly6C^+$ monocytes, 38% $BrdU^+MHC\text{-}II^{hi}$ immature TAM, 11% $BrdU^+MHC\text{-}II^{lo}$ immature TAM) and mature $MHC\text{-}II^{hi}$ and $MHC\text{-}II^{lo}$ TAM show a lag phase relative to immature macrophages (at 48 hours: 76% $BrdU^+$ immature macrophages, 14% $BrdU^+MHC\text{-}II^{hi}$ TAM, 9% $BrdU^+MHC\text{-}II^{lo}$ TAM), proposing a $Ly6C^{hi}$ monocyte → $MHC\text{-}II^{lo}$ and $MHC\text{-}II^{hi}$ immature TAM → $MHC\text{-}II^{lo}$ and $MHC\text{-}II^{hi}$ TAM differentiation scheme. By day 7, 79% of $MHC\text{-}II^{hi}$ TAM are $BrdU^+$ compared with only 67% $MHC\text{-}II^{lo}$ TAM, suggesting a somewhat faster turnover rate of the former population.

Because both TAM populations were derived from the same precursor, we next assessed their intratumoral localization. The hypoxia tracer pimonidazole was injected in tumor-bearing mice and 2 hours later intracellular hypoxyprobe staining was performed on tumor single-cell suspensions. Immature $MHC\text{-}II^{lo}$ macrophages and especially $MHC\text{-}II^{lo}$ TAM stained much brighter compared with their $MHC\text{-}II^{hi}$ counterparts (Fig. 2C). In line with these findings, $F4/80^+MHC\text{-}II^{hi}$ cells were located outside of hypoxyprobe $(HP\text{-}1)^+$ tumor regions in immunohistochemistry (Fig. 2D) and were not contained within the $HP\text{-}1^{hi}$ cell fraction in flow cytometry (Supplementary Fig. S3A). Conversely, the hypoxic regions in immunohistochemistry and the $HP\text{-}1^{hi}$ fraction in flow cytometry contained $F4/80^+$ cells that were mainly $MHC\text{-}II^{neg/lo}$. Moreover, by gating on the $CD11b^+Ly6G^-Ly6C^-$ (encompassing only mature TAM and TADC subsets) $HP\text{–}1^{high}$ versus $HP\text{-}1^{low}$ cells, a higher expression of MMR, IL-4Rα, and SR-A could be detected on the $HP\text{-}1^{high}$ fraction, corroborating the presence of the more M2-like

Published OnlineFirst November 12, 2013; DOI: 10.1158/0008-5472.CAN-13-1196

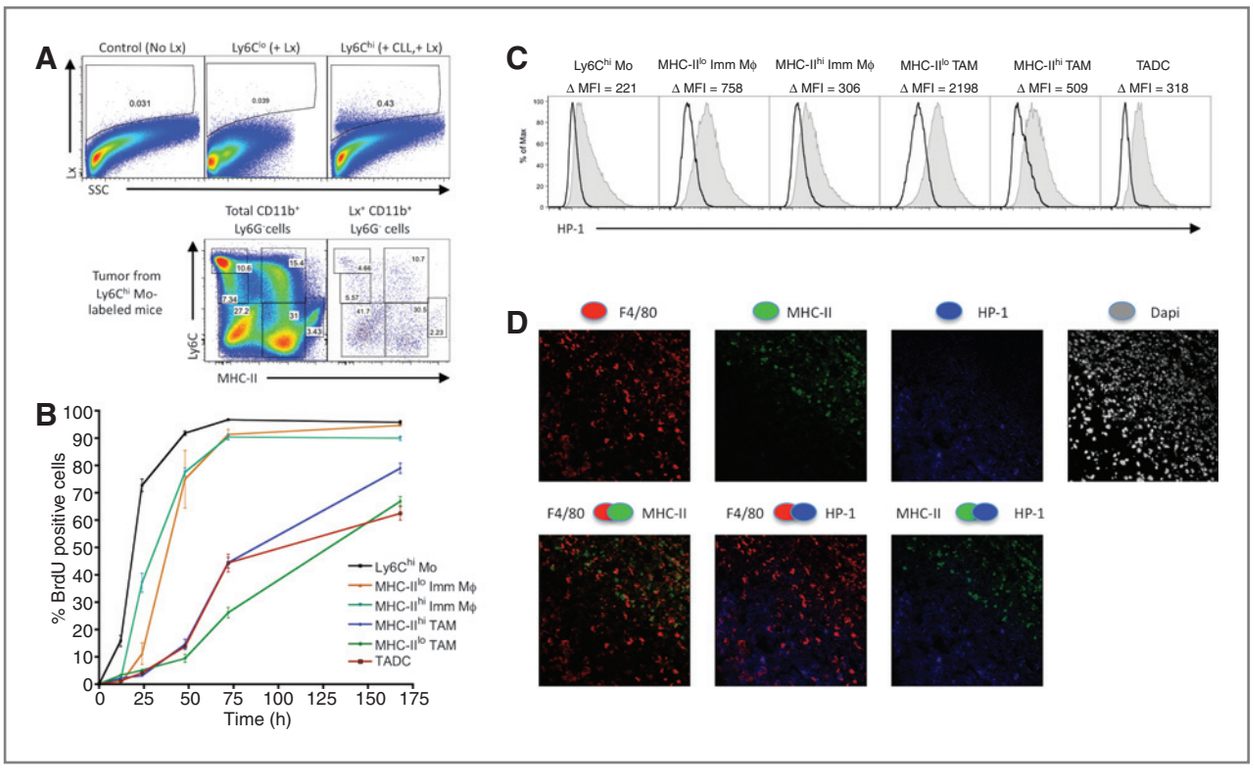

Figure 2. TAM subsets are derived from the same monocyte precursor but reside in differentially oxygenized tumor regions. A, the percentage of fluorescent latex$^+$ cells infiltrating 6-day-old 3LL-R tumors from untreated mice (No Lx) or from mice in which the Ly6C^{lo} (+Lx) or Ly6C^{hi} (+CLL+Lx) blood monocytes were labeled are shown. In addition, Ly6C versus MHC-II plots of the gated total CD11b$^+$Ly6G$^-$ population or the latex$^+$CD11b$^+$Ly6G$^-$ population within 3LL-R tumors (Ly6C^{hi} blood monocyte labeled) are shown. B, kinetics of BrdU incorporation in the distinct TAM subsets. Ten days 3LL-R tumor-bearing mice were left untreated (0 hour) or continuously given BrdU in the drinking water for the indicated time periods, after which tumors were collected. BrdU incorporation was measured using intracellular flow cytometry. The graph shows the percentage of BrdU$^+$ cells within the gated subpopulation after different time points of BrdU administration. C, 3LL-R tumor-bearing mice were left untreated (control) or were injected with pimonidazole (HP-1). Tumors were then collected and the presence of HP-1 adducts on gated TAM subsets was assessed using intracellular flow cytometry. ΔMFI = MFI HP1 − MFI control. D, frozen tumor sections from HP-1 injected mice were triple stained for F4/80, MHC-II, and HP-1 adducts. Nuclei were stained using DAPI. All experiments, $n \geq 6$.

MHC-II^{lo} TAM in this fraction. In conclusion, MHC-II^{lo} TAM rather associate with hypoxic regions, whereas MHC-II^{hi} TAM reside in less hypoxic areas.

Hypoxia does not define TAM differentiation and polarization, but specifically fine-tunes the molecular and functional profile of the MHC–II^{lo} TAM subset

To address whether hypoxia is the driving force behind TAM subset differentiation, 3LL-R tumors were inoculated in *PHD2*$^{+/-}$ mice. *PHD2*-haplodeficiency was shown before to foster vessel maturation and enhanced tumor oxygenation in several mouse tumor models without affecting primary tumor growth (13). Accordingly, overall oxygen pressure was significantly increased and the hypoxic HP-1$^+$ area significantly reduced in *PHD2*$^{+/-}$ 3LL-R tumors (Fig. 3A and B). Tumor perfusion (Supplementary Fig. S4B–S4D) and vessel coverage (Supplementary Fig. S4E–S4G) were also significantly higher in *PHD2*$^{+/-}$ tumors, whereas vessel density remained unchanged (Supplementary Fig. S4A), indicating that these vessels were more mature, tight, and stable. However, nearly no differences were observed at the level of myeloid cell infiltration, the relative abundance of MHC-II^{lo} and MHC-II^{hi} TAM, or the expression of prototypical M2 markers in these cells (Fig. 3C and D). Hence, hypoxia is not the main driver of TAM subset differentiation and polarization inside tumors.

We then assessed whether hypoxia contributes to a fine-tuning of the TAM phenotype. Corroborating their association with hypoxic regions, many of the hypoxia-dependent genes [*Vegfa, Angpt2, Flt1* (VEGFR1), *Kdr* (VEGFR2), *Egf, Slc2a1* (Glut1), *Slc2a3* (Glut3), *Ldha*, *Plau* (uPA), *Igf1*, *Serpine1* (PAI-1), *Nos2* (iNOS), and *Cxcl1* (KC)] were significantly upregulated in MHC-II^{lo} TAM compared with MHC-II^{hi} TAM in control tumors (Fig. 4A). Interestingly, genes regulating angiogenesis, metabolism, or cancer cell invasiveness such as *Vegfa*, *Slc2a1*, *Slc2a3*, *Serpine1*, *Plau*, *Nos2*, and *Cxcl1* were significantly downregulated in MHC-II^{lo} TAM from *PHD2*$^{+/-}$ tumors compared with MHC-II^{lo} TAM of control tumors. In contrast, the expression level of these hypoxia-regulated genes was less altered in MHC–II^{hi} TAM of both genotypes. Hence, hypoxia regulates the expression of a subset of genes mainly in the MHC-II^{lo} TAM population. For VEGF-A, GLUT-3, GLUT-1, and iNOS, these findings could be recapitulated at the protein level (Supplementary Fig. S5A and S5B). In agreement, the *in vivo* angiogenic activity of MHC-II^{lo} TAM from *PHD2*$^{+/-}$ tumors is significantly reduced as compared with their WT counterparts whereas this is not the case for MHC-II^{hi} TAM (Fig. 4B).

Published OnlineFirst November 12, 2013; DOI: 10.1158/0008-5472.CAN-13-1196

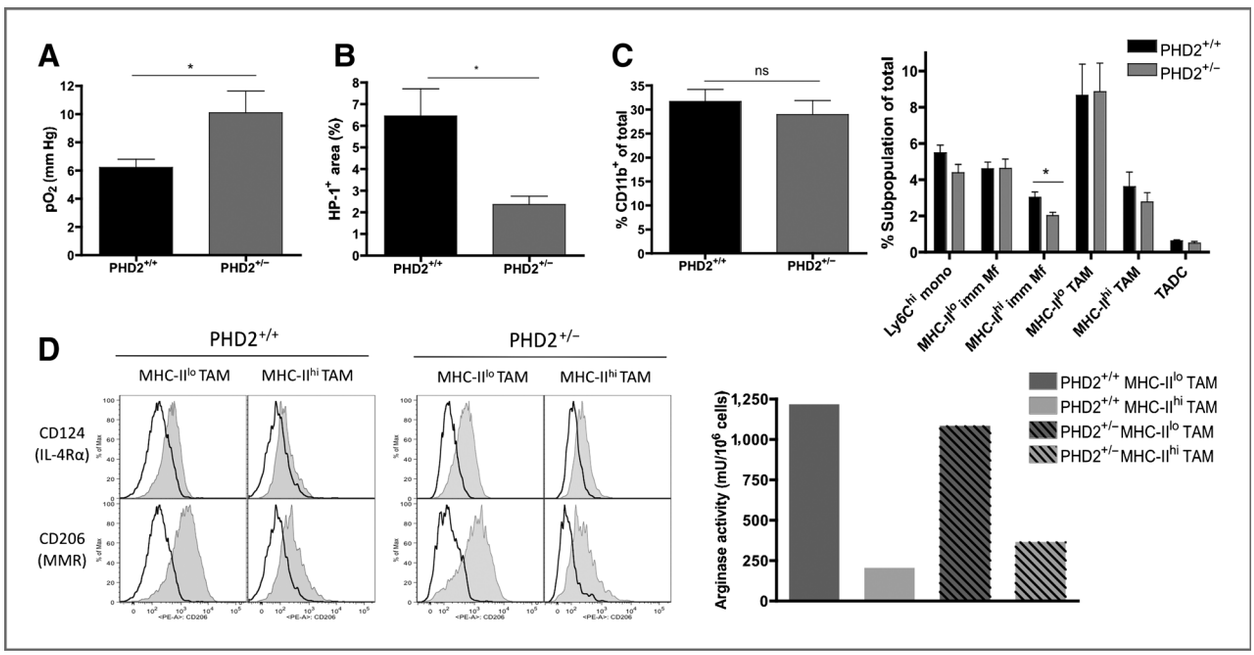

Figure 3. Characterization of 3LL-R tumors in *PHD2*$^{+/-}$ mice. 3LL-R tumors were grown for 12 days in *PHD2*$^{+/+}$ and *PHD2*$^{+/-}$ mice, after which intratumoral pO_2 (A) was measured via EPR oxymetry ($n = 5$) and morphometric quantification (B) of HP-1 staining on tumor slides was performed ($n = 5$). C, the percentage of CD11b$^+$ cells (within the total tumor single-cell suspension) and the percentage of mononuclear phagocyte subsets (within the gated CD11b$^+$ population) were determined ($n = 6$). D, surface marker expression for the M2 markers MMR and IL-4Rα on TAM of *PHD2*$^{+/+}$ and *PHD2*$^{+/-}$ tumors was assessed by flow cytometry. Shaded histogram, expression of the indicated marker; black line, isotype control. Arginase enzymatic activity was measured in lysates of 5×10^5 sorted TAM from a pool of 6 tumor-bearing mice.

A potential caveat for the interpretation of the results in *PHD2*$^{+/-}$ mice is the fact that also the macrophages in these mice are *PHD2*-haplodeficient, and hence experience a "genetic type" of hypoxia with a potential skewing of their activation state (14). Therefore, we inoculated 3LL-R in *PHD2*$^{+/+}$ → *PHD2*$^{+/-}$ bone marrow chimeric mice (microenvironmental haplodeficiency) versus *PHD2*$^{+/+}$ → *PHD2*$^{+/+}$ controls. Tumor hypoxic areas were smaller in the former (Fig. 4C), illustrating that *PHD2*-haplodeficiency in nonhematopoietic cells is sufficient to increase oxygenation. In line with the data in *PHD2*$^{+/-}$ mice, many hypoxia-regulated genes were significantly downregulated in MHC-II^{lo}, but not MHC-II^{hi}, TAM from tumors grown in *PHD2*$^{+/+}$ → *PHD2*$^{+/-}$ mice (Fig. 4D). These data corroborate the conclusion that environmental hypoxia mainly affects the MHC-II^{lo} TAM phenotype.

Discussion

TAM reside in a complex microenvironment, so their molecular and functional profile is under the influence of multiple factors. *In vivo* evidence exists for the role of immune cell- and cancer cell-derived factors (e.g., cytokines such as IL–4 and IL-10, immunoglobulins, prostaglandin E_2, exosomes) in shaping the protumoral functions of TAM during tumor progression (15,16). However, the impact of tumor hypoxia (0.1–3% O_2) is less clear in this respect, despite the known association of macrophages with hypoxic regions (4–7).

Indeed, our data demonstrate the existence of at least 2 main TAM subsets, discriminated mainly by the differential MHC–II expression level, in subcutaneous and orthotopic lung carcinomas. Hereby the MHC-II^{lo} subpopulation resides in more hypoxic regions as illustrated by intracellular FACS staining and immunohistochemistry upon pimonidazole treatment of the tumors. Earlier findings also pointed to the coexistence of TAM within hypoxic and less hypoxic regions in models of mouse mammary (4, 5) and human prostate carcinoma (6). The molecular mechanisms responsible for the guidance of TAM toward hypoxic areas are not entirely clear, but it has been shown that the angiopoietin-2/Tie2 interaction regulates the vascular proximity of MMR$^+$Tie2$^+$ macrophages (17). Importantly, both TAM subsets derive from a common Ly6C^{hi} monocyte precursor that continuously seeds the tumor, suggesting that distinct intratumoral cues drive the differentiating monocytes either to an MHC-II^{lo} or MHC-II^{hi} phenotype. One of the outstanding questions was whether hypoxia itself is the driving force behind this dichotomous monocyte differentiation. In addition, hypoxic MHC-II^{lo} TAM express higher levels of prototype M2 markers such as MMR, IL-4Rα, and arginase, and it was unclear whether this activation state is regulated by oxygen deprivation.

We used *PHD2*-haplodeficient mice as a tool to directly alter oxygen availability in the tumor. Mazzone and colleagues (13) had demonstrated that the tumor vessels in these mice are more mature, increasing oxygen transport to the tumor, and that an endothelial cell-restricted *PHD2*-haplodeficiency is sufficient to drive this phenomenon. In agreement with these findings, oxygen pressure increases and the hypoxic area diminishes in 3LL-R tumors grown in *PHD2*$^{+/-}$ mice, as well as in *PHD2*$^{+/+}$ → *PHD2*$^{+/-}$ chimeras. It is important to note

Published OnlineFirst November 12, 2013; DOI: 10.1158/0008-5472.CAN-13-1196

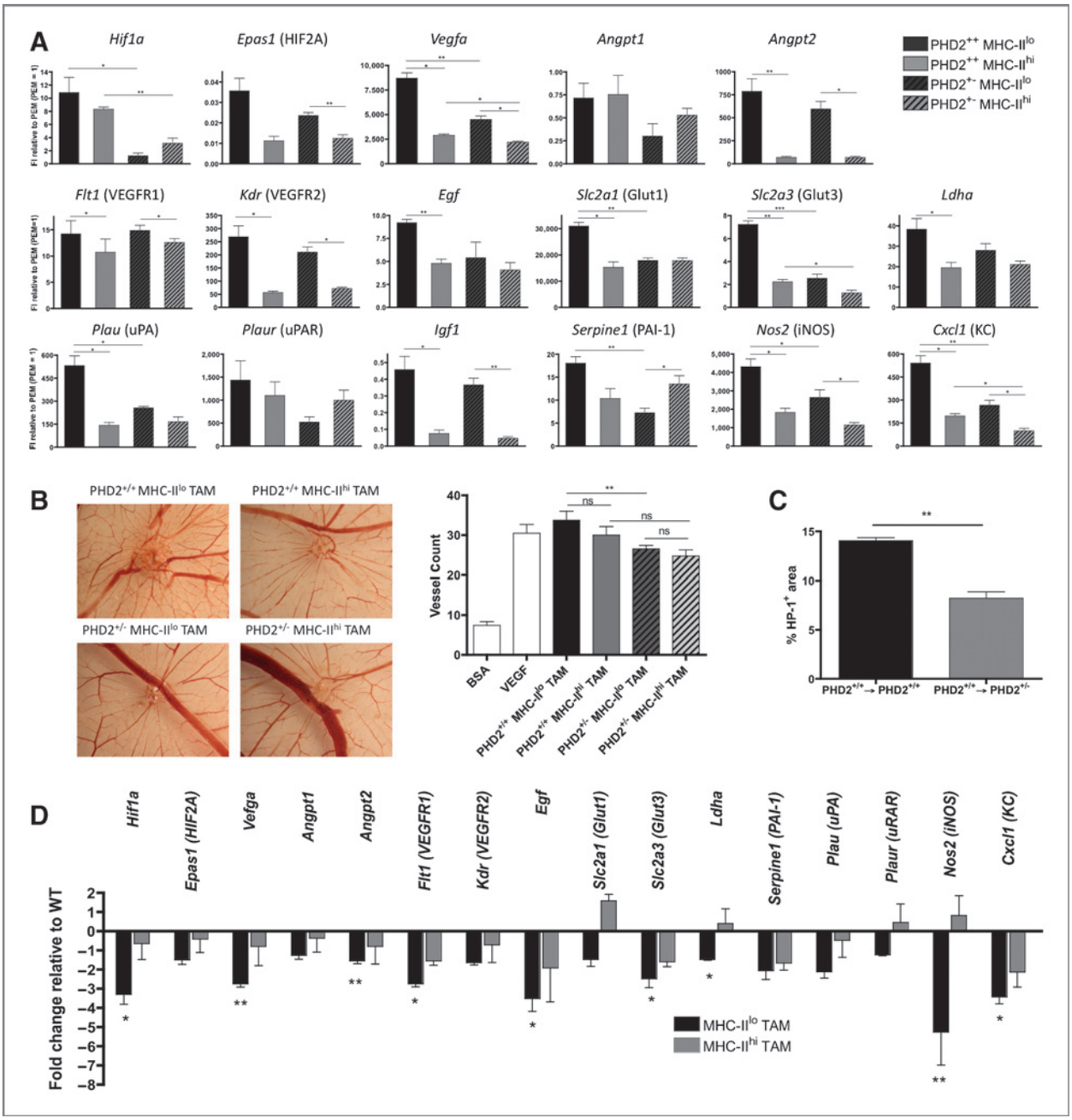

Figure 4. Influence of environmental hypoxia on the gene expression profile and angiogenic activity of TAM subsets. A, expression of hypoxia-regulated genes in sorted MHC-II^{lo} and MHC-II^{hi} TAM from 13-day-old 3LL-R tumors grown in *PHD2*$^{+/-}$ or *PHD2*$^{+/+}$ mice was assessed using qRT-PCR. The expression of each gene was normalized based on the S12 housekeeping gene and is shown as the fold induction compared with the expression in sorted peritoneal macrophages. B, sorted MHC-II^{lo} and MHC-II^{hi} TAM from 12-day-old 3LL-R tumors grown in *PHD2*$^{+/-}$ and *PHD2*$^{+/+}$ mice were grafted on the developing chorioallantoic membrane from fertilized chicken eggs. BSA and rhVEGF were used as negative and positive controls, respectively. The number of vessels growing toward the implants was quantified and this region was photographed. Values are the mean number of implant-directed vessels ± SEM. C, tumor sections from 3LL-R tumors grown in *PHD2*$^{+/+}$ → *PHD2*$^{+/-}$ and control *PHD2*$^{+/+}$ → *PHD2*$^{+/+}$ bone marrow chimeras were frozen upon HP-1 injection and were stained for HP-1 adducts and DAPI. Mean % HP-1 area ± SEM are given. D, gene expression of sorted MHC-II^{lo} and MHC-II^{hi} TAM grown in *PHD2*$^{+/+}$ → *PHD2*$^{+/-}$ bone marrow chimeras. Expression levels were first normalized based on the S12 gene and calculated as the fold induction compared with the expression in sorted peritoneal macrophages. Bars represent the up- or downregulation of the expression of the indicated genes, compared with the corresponding TAM subset in control bone marrow chimeras. All experiments, $n \geq 3$. *, $P < 0.05$; **, $P < 0.01$; ***, $P < 0.001$.

that this approach more directly assesses the overall impact of hypoxia on tumor macrophages, in contrast to studies where macrophages were engineered to lack only HIF-1α or HIF-2α (18,19). Moreover, HIFs also act on gene transcription in a hypoxia-independent fashion, whereby HIF-1α is induced by Th1 cytokines in pro-inflammatory M1 macrophages and

Published OnlineFirst November 12, 2013; DOI: 10.1158/0008-5472.CAN-13-1196

HIF-2α by Th2 cytokines in M2 macrophages (20). Our findings in *PHD2*-haplodeficient mice demonstrate that the tumor oxygenation state does not significantly alter the attraction of monocytes to the tumor nor the efficiency of monocyte differentiation into M2-like MHC-II^{lo} or M1-like MHC-II^{hi} TAM. Reduced hypoxia also does not seem to affect the expression of such M2-markers as MMR, IL-4Rα, and arginase in MHC-II^{lo} TAM, but rather downregulates their expression of typical hypoxia-responsive genes involved in glycolysis (*Slc2a1*, *Slc2a3, Ldha*), angiogenesis (*Vegfa, Angpt1, Angpt2, Kdr, Nos2, Cxcl1*), and metastasis (*Egf, uPA, uPAR, Igf1, Serpine1*). These results were phenocopied in *PHD2*$^{+/+}$ → *PHD2*$^{+/-}$ chimeras, illustrating that the *PHD2*-haplodeficiency in macrophages does not majorly account for the observed changes in gene expression.

Together, our data suggest a model whereby tumor-infiltrating Ly6C^{hi} monocytes either become MHC-II^{lo} M2-like TAM or MHC-II^{hi} M1-like TAM under the influence of microenvironmental stimuli other than hypoxia. Once formed, MHC-II^{lo} TAM are preferentially attracted to hypoxic regions where they upregulate hypoxia-regulated genes and their angiogenic capacity. By contrast, MHC-II^{hi} TAM remain largely unaffected by hypoxia.

Disclosure of Potential Conflicts of Interest

No potential conflicts of interest were disclosed.

Authors' Contributions

Conception and design: D. Laoui, K. Movahedi, P. De Baetselier, M. Mazzone, J.A. Van Ginderachter

Development of methodology: K. Movahedi, I. Houbracken, O. Karroum, J.A. Van Ginderachter

Acquisition of data (provided animals, acquired and managed patients, provided facilities, etc.): D. Laoui, E. Van Overmeire, G. Di Conza, C. Aldeni, J. Keirsse, Y. Morias, I. Houbracken, E. Schouppe, Y. Elkrim, O. Karroum, B. Jordan, C. Gysemans, M. Mazzone

Analysis and interpretation of data (e.g., statistical analysis, biostatistics, computational analysis): D. Laoui, G. Di Conza, C. Aldeni, I. Houbracken, B. Jordan, C. Gysemans, M. Mazzone, J.A. Van Ginderachter

Writing, review, and/or revision of the manuscript: D. Laoui, P. De Baetselier, M. Mazzone, J.A. Van Ginderachter

Administrative, technical, or material support (i.e., reporting or organizing data, constructing databases): I. Houbracken, Y. Elkrim, P. Carmeliet, C. Gysemans, P. De Baetselier

Study supervision: P. De Baetselier, M. Mazzone, J.A. Van Ginderachter

Grant Support

This work was supported by a doctoral grant from IWT-Vlaanderen to D. Laoui and Y. Morias, a scholarship from "Stichting Emmanuel van der Schueren" to D. Laoui, J. Keirsse, K. Movahedi, and E. Schouppe, a doctoral grant from FWO-Vlaanderen to E. Van Overmeire, G. Di Conza, K. Movahedi, and E. Schouppe, a grant from "Stichting tegen Kanker" to P. De Baetselier and J.A. Van Ginderachter, and M. Mazzone is supported by an ERC starting grant (OxyMo).

The costs of publication of this article were defrayed in part by the payment of page charges. This article must therefore be hereby marked *advertisement* in accordance with 18 U.S.C. Section 1734 solely to indicate this fact.

Received April 23, 2013; revised September 30, 2013; accepted October 17, 2013; published OnlineFirst November 12, 2013.

References

1. Qian BZ, Pollard JW. Macrophage diversity enhances tumor progression and metastasis. Cell 2010;141:39–51.
2. Laoui D, Van Overmeire E, Movahedi K, Van den Bossche J, Schouppe E, Mommer C, et al. Mononuclear phagocyte heterogeneity in cancer: different subsets and activation states reaching out at the tumor site. Immunobiology 2011;216:1192–202.
3. Lewis CE, Pollard JW. Distinct role of macrophages in different tumor microenvironments. Cancer Res 2006;66:605–12.
4. Movahedi K, Laoui D, Gysemans C, Baeten M, Stange G, Van den Bossche J, et al. Different tumor microenvironments contain functionally distinct subsets of macrophages derived from Ly6C(high) monocytes. Cancer Res 2010;70:572839.
5. Wyckoff JB, Wang Y, Lin EY, Li J, Goswami S, Stanley ER , et al. Direct visualization of macrophage-assisted tumor cell intravasation in mammary tumors. Cancer Res 2007;67:2649–56.
6. Muthana M, Giannoudis A, Scott SD, Fang H, Coffelt SB, Morrow FJ, et al. Use of macrophages to target therapeutic adenovirus to human prostate tumors. Cancer Res 2011;71:1805–15
7. Movahedi K, Schoonooghe S, Laoui D, Houbracken I, Waelput W, Breckpot K, et al. Nanobody-based targeting of the macrophage mannose receptor for effective *in vivo* imaging of tumor-associated macrophages. Cancer Res 2012;72:4165–4177.
8. Osinsky S, Bubnovskaya L, Ganusevich I, Kovelskaya A, Gumenyuk L, Olijnichenko G , et al. Hypoxia, tumour-associated macrophages, microvessel density, VEGF and matrix metalloproteinases in human gastric cancer: interaction and impact on survival. Clin Transl Oncol 2011;13:133–38.
9. Burke B, Giannoudis A, Corke KP, Gill D, Wells M, Ziegler-Heitbrock L, et al. Hypoxia-induced gene expression in human macrophages, implications for ischemic tissue and hypoxia-regulated gene therapy. Am J Pathol. 2003;163:1233–43.
10. Cramer T, Yamanishi Y, Clausen BE, Förster I, Pawlinski R, Mackman N, et al. HIF-1a is essential for myeloid cell-mediated inflammation. Cell 2003;112:645–57.
11. Fang H, Hughes R, Murdoch C, Coffelt C, Biswas SK, Harris AL , et al. Hypoxia inducible factors 1 and 2 are important transcriptional effectors in primary macrophages experiencing hypoxia. Blood 2009;144:844–59.
12. Hamilton JA, Lacey DC, Turner A, de Kok B, Huynh J, Scholz GM. Hypoxia enhances the proliferative response of macrophages to CSF-1 and their pro-survival response to TNF. PLoS One 2012;7:e45853.
13. Mazzone M, Dettori D, Leite de Oliveira R, Loges S, Schmidt T, Jonckx B , et al. Heterozygous deficiency of PHD2 restores tumor oxygenation and inhibits metastasis via endothelial normalization. Cell 2009;136:839–51
14. Takeda Y, Costa S, Delamarre E, Roncal C, Leite de Oliveira R, Squadrito ML , et al. Macrophage skewing by Phd2 haplodeficiency prevents ischaemia by inducing arteriogenesis. Nature 2011;479:122–6.
15. Ruffell B, Affara NI, Coussens LM. Differential macrophage programming in the tumor microenvironment. Trends Immunol 2012;33:119–26.
16. Schouppe E, De Baetselier P, Van Ginderachter JA, Sarukhan A. Instruction of myeloid cells by the tumor microenvironment: open questions on the dynamics and plasticity of different tumor-associated myeloid cell populations. OncoImmunol 2012;1:1135–45
17. Mazzieri R, Pucci F, Moi D, Zonari E, Ranghetti A, et al. Targeting the ANG2/TIE2 axis inhibits tumor growth and metastasis by impairing angiogenesis and disabling rebounds of proangiogenic myeloid cells. Cancer Cell 2011;19:512–26.
18. Doedens AL, Stockmann C, Rubinstein MP, Liao D, Zhang N, DeNardo DG, et al. Macrophage expression of hypoxia-inducible factor-1α suppresses T-cell function and promotes tumor progression. Cancer Res 2010;70:7465–75.
19. Imtiyaz HZ, Williams EP, Hickey MM, Patel SA, Durham AC, Yuan LJ, et al. Hypoxia-inducible factor 2α regulates macrophage function in mouse models of acute and tumor inflammation. J Clin Invest 2010;120:2699–14.
20. Takeda N, O'Dea EL, Doedens A, Kim JW, Weidemann A, Stockmann C , et al. Differential activation and antagonistic function of HIF-α isoforms in macrophages are essential for NO homeostasis. Genes Dev 2011;24:491–501.

Published OnlineFirst November 12, 2013; DOI: 10.1158/0008-5472.CAN-13-1196

Cancer Research
The Journal of Cancer Research (1916–1930) | The American Journal of Cancer (1931–1940)

AACR American Association for Cancer Research

Tumor Hypoxia Does Not Drive Differentiation of Tumor-Associated Macrophages but Rather Fine-Tunes the M2-like Macrophage Population

Damya Laoui, Eva Van Overmeire, Giusy Di Conza, et al.

Cancer Res 2014;74:24-30. Published OnlineFirst November 12, 2013.